



Role of mixed molecular weight PEO-PVDF polymers in improving the ionic conductivity of blended solid polymer electrolytes

C Revathy¹ · V R Sunitha² · Benson K. Money² · Rex Joseph¹ · S. Radhakrishnan³

Received: 30 March 2023 / Revised: 4 July 2023 / Accepted: 22 July 2023 / Published online: 3 August 2023
© The Author(s), under exclusive licence to Springer-Verlag GmbH Germany, part of Springer Nature 2023

Abstract

Blended solid polymer electrolytes (BSPE) were prepared by mixing different molecular weight polymers PEO₆ ($M_w = 1 \times 10^6$ g/mol), PEO₅ ($M_w = 1 \times 10^5$ g/mol), and PVDF ($M_w = 5.25 \times 10^5$ g/mol) complexed with lithium salt. Conductivity and dielectric studies at different temperatures were carried out on these BSPE systems by varying the wt% of PEO₅ and PVDF with respect to PEO₆, keeping the wt% of lithium salt constant. The electrical characterizations of BSPE systems have been investigated using impedance spectroscopy in the frequency range 0.1–10⁶ Hz. The conductivity data shows that inclusion of PEO₅ and PVDF into the PEO₆ matrix improved the overall lithium-ion dynamics in the polymer matrix. The composition, PEO₆ (94 wt%)-PEO₅ (3 wt%)/PVDF (3 wt%)-LiClO₄, exhibited maximum conductivity of 6.44×10^{-4} Scm⁻¹ at 303 K. The DC conductivity variation with temperature of BSPE systems follows Arrhenius relation and variation of AC conductivities with frequency obeys Jonscher's power law. The real and imaginary part of dielectric constant and the dielectric relaxation were also investigated.

Keywords Blend polymer electrolyte · Ionic conductivity · Ion hopping rate · Ion concentration factor · Dielectric constant · Dielectric relaxation

Introduction

Solid polymer electrolytes have received considerable attention because of their safety, flexibility, processability, and electrochemical stability [1, 2]. Polymers, which have long –[C–H₂–]– backbones and dynamic chains with high salt dissolving capability and ability to donate sufficient electrons to form coordination with cations, are preferred over other amorphous systems [3–5].

In general, poly(ethylene oxide) (PEO), having both crystalline and amorphous phases, is highly preferred, as it

satisfies most of the requirements of a solid polymer electrolyte [6]. The highly flexible macromolecular chains in PEO not only help in the cation movement but also exhibit high mechanical and electrochemical stability [1]. However, PEO-based polymer electrolytes suffer from low ionic conductivities at ambient temperature; hence, the amorphous phase of PEO needs to be enhanced to improve the ionic conductivity [1–5]. Numerous techniques such as incorporation of layered silicates, nanofillers, low molecular weight plasticizers, and blending with various kinds of polymers have been adopted to enhance the amorphous phase and hence the conductivity [7, 8].

One of the simple and cost-effective methods to improve conductivity is to blend two or more polymers of different molecular weights. Polymer blend technique is a viable method as physical properties of the compositions can be controlled easily, helps to suppress the drawback of individual polymers, and enhances their useful properties [8–11]. However, the blending of polymer of different molecular weights does not change the chemical structure and chain of the polymer like in polymerization [12].

Various studies have reported that, when PEO-based polymer is blended with other polymers, they exhibited ionic

✉ V R Sunitha
sunitha.vr@christuniversity.in

S. Radhakrishnan
sradhakrishnan@pes.edu

¹ Department of Electrical & Electronics Engineering, PES University, -560085, Bangalore, Karnataka, India

² Department of Sciences and Humanities, School of Engineering and Technology, Christ (Deemed to be University), -560074, Bangalore, Karnataka, India

³ Department of Science and Humanities, PES University, -560085, Bangalore, Karnataka, India

conductivity of the order of $\sim 10^{-12}$ to $\sim 10^{-5}$ Scm^{-1} at room temperature [5, 6, 9, 13]. It is also observed that PEO with poly(methylmethacrylate) (PMMA), poly(vinyl pyrrolidone) (PVP), poly(vinylidene fluoride) (PVDF), and poly(vinyl acetate) (PVAc) exhibited improved segmental motion of polymer, higher salt dissociation, and faster Li^+ transportation and also enhanced the mechanical and thermal stability of polymer electrolytes [4–8].

In the present study, we report the effect of blending PEO of two different molecular weights with PVDF. The high molecular weight PEO is used as the host matrix. PVDF is known to have high dielectric constants, low dissipation factor, and good chemical, mechanical, and thermal stability. Further PVDF also helps to reduce the crystallinity of PEO-based systems [13, 14]. A small amount of PEO with lesser molecular weight is found to help blending the PVDF effectively into the system.

It is reported that lithium perchlorate, LiClO_4 , (-less hygroscopic and stable at environmental conditions as compared to other Li salts) promotes higher salt dissociation and thus provides a greater number of ions [15, 16]. Further, LiClO_4 is highly soluble in most of the organic solvents, dissociates easily, and helps in reducing the crystalline phase of the polymer backbone. This also lowers the energy barrier for segmental motion which is crucial to ion conduction [16–19]. Presence of high Li^+ ion coordination with oxygen present in the PEO helps in Li^+ ion transportation [1] whereas fluorine in the PVDF is unstable with Li^+ ions, leading to poor stability and lower performance [16, 20, 21]. It is reported that inclusion of lesser molecular weight PEO

is also an effective way to enhance the conductivity of PEO-based systems [22].

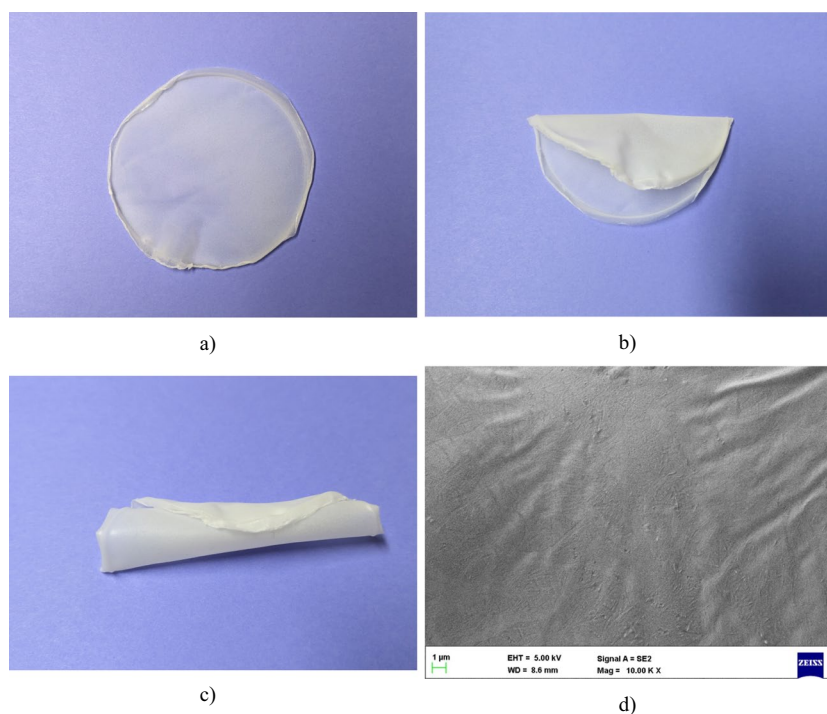
Materials and methods

Preparation of blended solid polymer electrolyte

BSPE compositions were prepared by varying the PEO_6 ($M_w = 1 \times 10^6$ g/mol), PEO_5 ($M_w = 1 \times 10^5$ g/mol), and PVDF ($M_w = 5.25 \times 10^5$ g/mol) keeping the lithium salt concentration constant (20 wt%). The PEO_6 dissolved in acetonitrile (ACN) was blended with PEO_5 and PVDF mix (which were dissolved separately in ACN and N-methyl-2-pyrrolidone (NMP), respectively). The solutions were mixed and stirred for about 12 h to attain homogeneity. To this homogenous solution, desired amount of lithium perchlorate (LiClO_4) salt was dispersed. To ensure the even dispersion, the solution was latter sonicated using a digital ultrasonicator, followed by constant stirring for about 24 h. The obtained viscous solution was casted on a Petri dish and then transferred to hot air oven, maintained at 30°C , for 24 h in order to evaporate solvents slowly, thus resulting in a free-standing and flexible polymer film (Fig. 1a–c). Figure 1d shows the SEM image of optimal composition P3 which illustrates the film consistency. The dried samples were stored in glove box for further testing. The following compositions of blend systems were prepared using the above technique:

1. PEO:Li – 100 wt% PEO_6

Fig. 1 Blended solid polymer electrolyte sample **a** free standing film, **b** flexibility of film, **c** rollability of film, and **d** SEM image of composition P3 at $\times 10000$ magnification



2. P1 – 98 wt% PEO₆ + 1 wt% PEO₅ + 1 wt% PVDF
3. P2 – 96 wt% PEO₆ + 2 wt% PEO₅ + 2 wt% PVDF
4. P3 – 94 wt% PEO₆ + 3 wt% PEO₅ + 3 wt% PVDF
5. P4 – 92 wt% PEO₆ + 4 wt% PEO₅ + 4 wt% PVDF
6. P5 – 90 wt% PEO₆ + 5 wt% PEO₅ + 5 wt% PVDF

Characterization

X-ray diffraction (XRD) studies were carried using Cu-K_α radiation of wavelength 1.5406 Å using SmartLab X-Ray Diffractometer, in the range 10° to 40° at a scanning rate of 0.02° s⁻¹ in order to analyze the crystallinity of prepared samples [4, 9]. The interactions between the polymers and salt were analyzed with Perkin Elmer Fourier Transform Infrared (FTIR) spectrometer in the wave number range 650 to 4000 cm⁻¹ with resolution of 1 cm⁻¹ [23]. Thermal analysis of pure PEO, PVDF, and BSPE systems have been performed, in order to see the change in the phase transition temperatures and enthalpy of melting, using Shimadzu DSC-60 Differential Scanning Calorimetry (DSC) in the range of 30 to 100 °C with heating rate of 10 °C min⁻¹ under inert (N₂) atmosphere [2, 4]. The relative percentage of crystallinity (χ_c) in the BSPE systems were estimated using the relation $\chi_c = \frac{\Delta H_m}{\Delta H_0} \times 100\%$ where ΔH_m is the enthalpy of melting of various composition and ΔH_0 is the enthalpy of melting of PEO₆ [24, 25].

The electrical characterization of the BSPE systems were carried out on Keithley source meter 2400 and CHI608D electrochemical workstation. The ion transport numbers of the BSPE systems were evaluated using Wagner's polarization technique [26, 27], and it was found to be between 0.90 and 0.97. This implies that the charge transport in these system is mainly due to the movement of ions [28]. An equivalent circuit model for the compositions was modelled using Electrochemical Impedance Spectroscopy (EIS) spectrum analyzer software (open source).

Results and discussion

XRD analysis

Figure 2 shows XRD spectra of BSPE systems. All the XRD patterns show two prominent Bragg peaks around $2\theta \sim 19.14^\circ$ and 23.24° with a diffused background. This indicates the semi-crystalline phase of PEO polymer from (120) and (112) plane, respectively [29]. The low intense peaks at $2\theta \sim 26.17^\circ$, 27.86° , 36.19° , and 39.72° correspond to α phase of PVDF [13, 14]. The β phase of PVDF was not observed in the blend systems due to the relatively

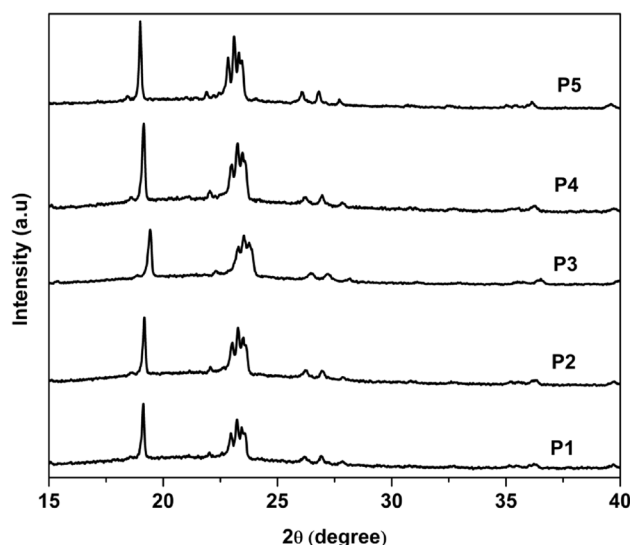


Fig. 2 XRD patterns of the BSPE systems

Table 1 d-spacing and crystallite sizes of the BSPE systems

Composition	Peak 1 @ 19°		Peak 2 @ 23°	
	d-spacing (Å)	Scherrer length (nm)	d-spacing (Å)	Scherrer length (nm)
P1	4.64	64.76	3.83	12.11
P2	4.63	60.14	3.82	11.77
P3	4.56	49.54	3.78	11.77
P4	4.64	60.13	3.82	12.11
P5	4.67	70.14	3.85	12.28

low wt% of PVDF. The change in peak intensities and shift of these peaks reveals the interaction of PEO₅ and PVDF polymers in the modification of ordered arrangement of PEO₆ polymer [29]. It is observed that with addition of PEO₅ and PVDF polymers, the width of the prominent peaks were increasing with reduction in intensities. The composition P3 achieved maximum broadening and less intensity compared to the other compositions. No significant peaks corresponding to LiClO₄ were observed, which implies the absence of excess salt in the blended system [6, 30]. The crystallite size (Scherrer length) and d-spacing of various compositions were estimated using Scherrer equation [31], and the values are tabulated in Table 1. It is observed that, with the increase in the wt% of PEO₅ and PVDF, the d-spacing and crystallite size decrease up to composition P3. The reduction in crystallite size indicates the enhancement of amorphous phase in the BSPE systems. Further addition of higher wt% of PEO₅ and PVDF resulted in increase of d-spacing and crystallite sizes (Table 1).

Different scanning calorimetry analysis

Figure 3 shows the DSC thermograms of pure PEO, PVDF, and BSPE systems. The thermal parameters, i.e., melting temperature (T_m), enthalpy of melting (ΔH_m), and percentage of crystallinity (χ_c) of polymers, obtained from the DSC measurements, are tabulated in Table 2. The sharp endothermic peak at 70.43 °C corresponds to the melting temperature (T_m) of pure PEO₆. On the addition of PEO₅ and PVDF, the melting peak gets broaden and shifts towards the lower temperature, with the composition P3 exhibiting the lowest melting temperature (Table 2). However, it was observed that the further addition of PEO₅ and PVDF polymers increased the melting temperature shown in Table 2. Also, the composition P3 exhibited least percentage crystallinity among all the prepared samples. The lower percentage of crystallinity and melting temperature for composition P3 indicate an improvement in the amorphous phase of the polymer, which is also confirmed by XRD results. The enhancement in amorphous phase is associated with highly flexible polymer chains, leading to improved ion mobility [25, 32–34].

FTIR analysis

The FTIR spectra of pure PEO and BSPE systems are shown in Fig. 4a, b. From the figure, it is observed that various composition of polymer blends exhibited significant change in the peak positions, vibrational band intensities, band widths, and even emergence of new peaks. In all the compositions, the peak observed at 1640 cm⁻¹ represents vibration band of LiClO₄, and the peaks at 652 cm⁻¹ and 1093 cm⁻¹ represent internal vibration mode and antisymmetric stretching mode of ClO₄⁻ [35, 36]. The peaks observed at 839 cm⁻¹, 1282 cm⁻¹, and 1341 cm⁻¹ show CH₂ rocking, twisting, and wagging of PEO chain, respectively [37]. Peaks at 944 cm⁻¹, 1306 cm⁻¹, and 1504 cm⁻¹

Table 2 Melting temperature, enthalpy of melting, and % crystallinity of pure PEO and BSPE systems

Composition	T_m (°C)	ΔH_m (J/g)	χ_c (%)
PEO	70.44	64.06	100
P1	53.07	37.00	57.75
P2	50.42	33.80	52.76
P3	50.21	23.89	37.29
P4	56.58	35.60	55.57
P5	57.89	40.35	62.98

confirm the presence of PVDF in the polymer blend systems. The peaks at 944 cm⁻¹ and 1306 cm⁻¹ represent C=C bending and CF stretching of PVDF, respectively [13, 14]. The band appearing around 3472 cm⁻¹ represents OH stretching, and it is seen that peak broadens with increase in PVDF concentration [38]. The PEO exhibits characteristic triplet peaks at 1060 cm⁻¹, 1093 cm⁻¹, and 1144 cm⁻¹ [32]. The triplet peaks broaden whereas the peaks at 1060 cm⁻¹ and 1144 cm⁻¹ vanish as PVDF concentration increased. The new peak at 1504 cm⁻¹ indicates the deformation of CH₂, and the other characteristic peaks were also shifted for different compositions [23]. These changes imply polymer-polymer interaction and polymer salt interactions, which is also confirmed by the XRD and DSC results [32].

Figure 5 shows the FTIR spectra of composition P3 in the range of 1600 cm⁻¹ to 1680 cm⁻¹ that corresponds to LiClO₄ vibration. The spectra were deconvoluted to investigate the free ions and ion pair concentrations. The deconvolution clearly reveals the presence of two peaks at 1648 cm⁻¹ and 1668 cm⁻¹ (Fig. 5). The first peak is generally attributed to the presence of free ions and second peak to ion pairs [39, 40]. The fraction of free ions and ion pairs was calculated from area under the curve [36, 40–42]. The fraction of free ions for the optimal composition P3 was found to be 16% higher than the sample PEO:Li.

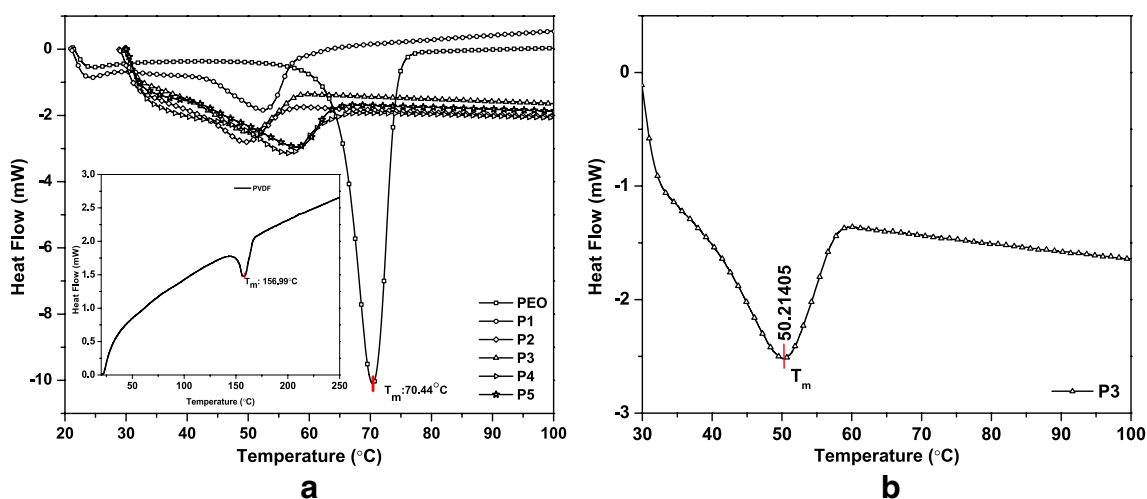


Fig. 3 a DSC plots for pure PEO, pure PVDF, and BSPE systems and b DSC plot of optimal composition P3

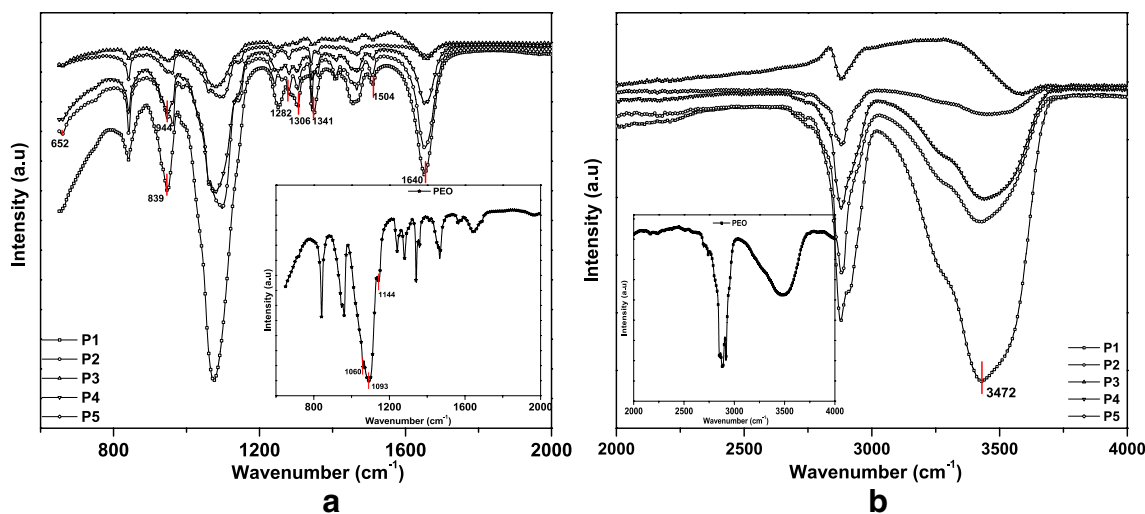


Fig. 4 FTIR spectra for pure PEO and BSPE system ranges **a** 650 cm^{-1} to 2000 cm^{-1} and **b** 2000 cm^{-1} to 4000 cm^{-1}

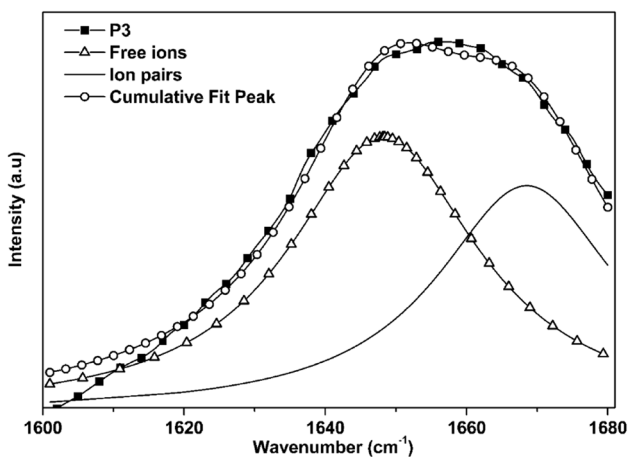


Fig. 5 FTIR-deconvoluted spectra of optimal composition P3 in the range of 1600 cm^{-1} to 1680 cm^{-1}

Impedance spectroscopic studies

Figure 6a shows the Nyquist plots for BSPE systems at 303 K. The plot consists of two distinct features, i.e., an incomplete semicircle and an inclined straight line. The intercept of the high frequency semicircle on the real axis (Z') represents bulk resistance (R_b), and the low frequency-inclined straight line shows the electrode polarization [19, 39, 40]. It was observed that among all the prepared samples, the composition P3 (96 wt% PEO₆ + 3 wt% PEO₅ + 3 wt% PVDF) exhibited lowest bulk resistance value at ambient temperature.

Figure 6b shows the impedance plots of the optimal composition (P3) at different temperatures. With increase in temperature, the intercept shifted towards lower side of the real Z' axis, i.e., the bulk resistance of the system

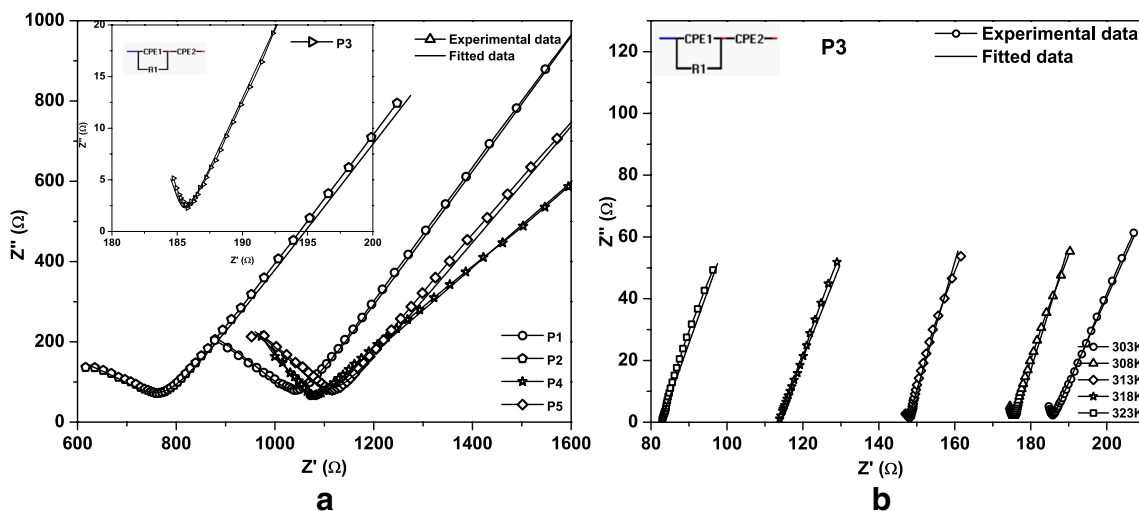


Fig. 6 Impedance plots of **a** BSPE systems at 303 K and **b** optimal composition P3 at different temperatures

decreases with increase in temperature [19]. Increase in temperature improves the chain flexibility and segmental motion of the amorphous phase which in turn decreases the bulk resistance of the system [6, 7].

Using EIS spectrum analyzer, the Nyquist plots of the BSPE systems and optimal composition (P3) were analyzed. All the data were fit to an electrical equivalent circuit (inset of Fig. 6a, b) that consists of parallel R1–CPE-1 (constant phase element) with an additional double layer capacitance CPE-2 in series, associated with electrode-electrolyte interface. The experimental data (open circles) coincide well with fit data (straight line) as seen in Fig. 6a, b. The bulk resistance and CPE-2 values of all the BSPE systems, from the fit parameters, are found to be in the range of 186 to 1116 Ω and 0.135 to 43 μF , respectively, at 303 K. The optimal composition P3 exhibited the lowest bulk resistance of 186 Ω and maximum CPE-2 of 43 μF , which is attributed to larger salt dissociation, greater ion mobility, and high charge accumulation at the electrode-electrolyte interfaces [41, 42].

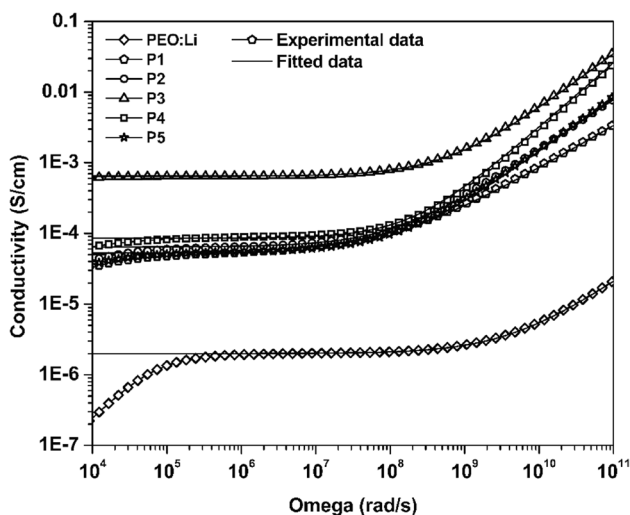


Fig. 7 Frequency-dependent conductivity of PEO:Li and BSPE systems at 303 K

Table 3 Jonscher's power law fitting and transport parameters, A , n , σ_{dc} , ω_H , and K for PEO:Li and BSPE systems at 303 K

Composition	σ_{dc} (Scm^{-1})	A	n	ω_H (s^{-1})	Concentration factor K (Scm^{-1} K s)
PEO:Li	2.03×10^{-6}	1.53×10^{-12}	0.74	1.88×10^8	3.27×10^{-12}
P1	5.22×10^{-5}	2.20×10^{-09}	0.50	5.63×10^8	2.81×10^{-11}
P2	6.37×10^{-5}	8.90×10^{-11}	0.67	6.37×10^8	3.03×10^{-11}
P3	6.44×10^{-4}	7.23×10^{-11}	0.78	8.13×10^8	2.4×10^{-10}
P4	8.77×10^{-5}	2.1×10^{-12}	0.91	2.37×10^8	1.12×10^{-10}
P5	5.37×10^{-5}	3.1×10^{-11}	0.77	1.27×10^8	1.29×10^{-10}

Frequency-dependent ionic conductivity

The frequency dependence of real part of conductivity, for PEO:Li and BSPE systems at 303 K, is shown in Fig. 7. It is seen that the variation of conductivity at low frequency region is independent of frequency whereas in the high frequency region, conductivity rises as the frequency increases, following the Jonscher's power law [43, 44].

The pre-exponential factor A , power law exponent n , DC conductivity σ_{dc} , and the ion hopping rate ω_H values were estimated using Jonscher's power law, and the values are tabulated in Table 3 [44–46]. It is observed that the DC conductivity, σ_{dc} , and ion hopping rate, ω_H , increased till 3 wt% PEO (Low Mw) + 3 wt% PVDF (optimal composition P3) which is comparable to similar blend systems reported with different salt compositions [1, 47–49]. In further addition of PEO₅ and PVDF, the ionic conductivity and ion hopping rate were found to be decreasing for the prepared BSPE systems.

Using Barton-Nakajima-Namikawa (BNN) relation, mobile ion concentration factor K was also estimated for PEO:Li and BSPE systems and is shown in Table 3 [44, 46]. The K factor was increased by two order magnitude for the optimal composition (P3) when compared with PEO:Li composition.

From the table, it is seen that σ_{dc} , ω_H , and K values increased with the addition of PEO₅ and PVDF. The enhancement observed in all these parameters could be attributed to the creation of free volume or voids due to large number of chain ends and entanglement of PEO₅ and PVDF. This in turn enhances the ion hopping conduction within the blend polymer chain dynamics [50, 51]. Apart from this, PEO₅ and PVDF polymers can also improve the salt dissociation and create flexible pathway within the blend system, thus facilitating better ion mobility [6]. However, at higher concentration of PEO₅ and PVDF, all these parameters were found to be decreasing. This is due to the increased viscosity of the blend systems, which hindered the ionic mobility and segmental motion [7, 16, 20].

Temperature-dependent ionic conductivity

The variation of $\log \sigma_{dc}$ as a function of temperature is plotted and shown in Fig. 8a. All the compositions exhibited linear behavior obeying Arrhenius relation [52–55]. It is seen that the conductivity of PEO:Li and BSPE systems increased with increase in temperature. As per the Arrhenius theory, polymer matrix expands on heating creating free volume for ionic movement and allows ions to move easily from one site to another. This in turn enhances the segmental motion of polymer and eases the translational ionic movement which can cause increased ionic conductivity [8, 56].

Using the Arrhenius plot, activation energy for PEO:Li and BSPE systems was evaluated and found to be between 0.491 and 0.198 eV (Fig. 8b). The optimal composition (P3) exhibited the least activation energy (0.198 eV). This clearly shows that the addition of PEO₅ and PVDF polymers helps the ions to overcome the energy barrier easily and thus enhancing the ionic conductivity [8].

Dielectric studies

The variation in dielectric constant and dielectric loss as a function of frequency for PEO:Li and BSPE systems at 303 K and 323 K are shown in Fig. 9a, b. It is observed that all

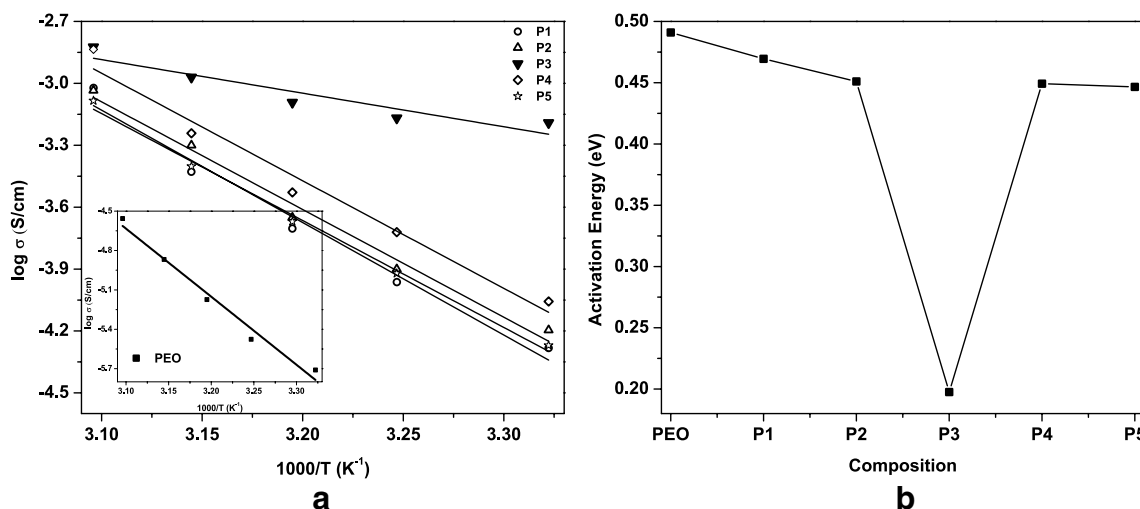


Fig. 8 a Temperature-dependent ionic conductivity of PEO:Li and BSPE systems and b variation of activation energy of PEO:Li and BSPE systems

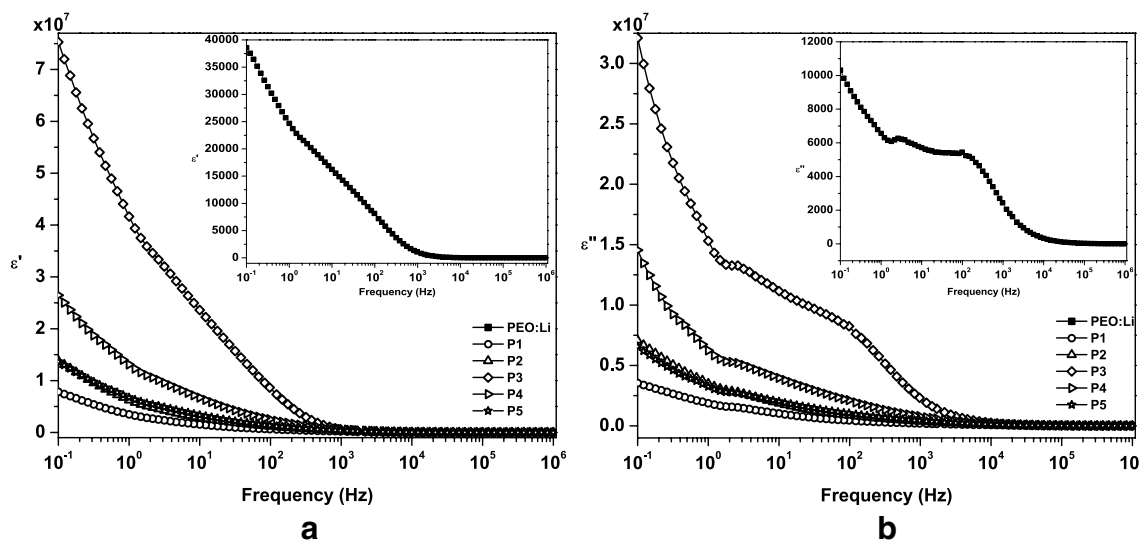
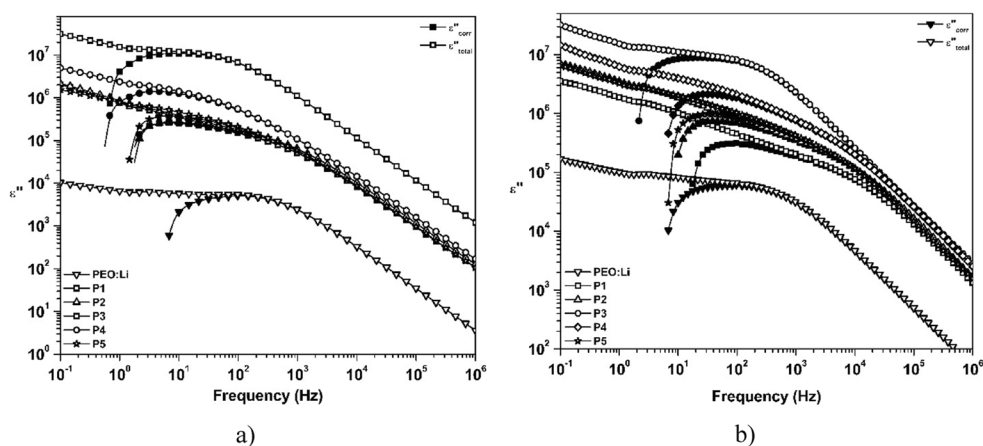


Fig. 9 Variation of a dielectric constant and b dielectric loss with frequency for PEO:Li and BSPE systems at 323 K

Fig. 10 Frequency-dependent $\epsilon''_{\text{total}}$ and ϵ''_{corr} of PEO:Li and BSPE systems at a 303 K and b 323 K



the compositions exhibited the similar dielectric behavior with respect to frequency. The higher value of dielectric constant and dielectric loss at low frequency is due to electrode polarization. At low frequencies, the dipoles have sufficient time to align themselves with respect to applied electric field. But as the frequency increases, the dipoles will not have sufficient time to align themselves along the field direction; hence, the value of dielectric constant reduces [37, 39]. It is also observed that with increase in temperature, dielectric constant and dielectric loss increase, since at higher temperature, free volume of the material increases which improves the structural dynamic of the polymer, polarization, and ion migration [37].

It is found that the optimal composition P3 exhibited the higher value of dielectric constant and dielectric loss due to higher dissociation of salt [42]. The variation in dielectric constant value in different composition confirms the effect of polymer blending which is also evident by DSC, XRD, and FTIR data.

Figure 9b shows the total dielectric loss $\epsilon''_{\text{total}}$, which generally consists of two parts, i.e., the bulk conductivity and the true dielectric loss. The peak appearing in the imaginary part of the dielectric loss spectra is due to the energy absorbed by the permanent dipoles in the samples. For polymer electrolyte with significant conductivity, the dielectric relaxation peaks may be hidden by the relaxation process of dipoles, originating from the polarization of mobile charge carrier present in the sample. So, in order to observe the true dielectric relaxation process, the observed $\epsilon''_{\text{total}}$ should be corrected by removing conductivity part using the relation $\epsilon''_{\text{corr}} = \epsilon''_{\text{total}} - \sigma_0/\epsilon_0\omega$ [57]. The obtained values of dielectric relaxation ϵ''_{corr} and the total dielectric loss $\epsilon''_{\text{total}}$ are plotted as a function of frequency for PEO:Li, and BSPE systems at 303 K and 323 K are shown in Fig. 10a, b. The ϵ''_{corr} peaks shifted towards lower frequency side of the spectra on addition of PEO₅ and PVDF polymers up to 3 wt% PEO₅ + 3 wt% PVDF (optimal composition P3). Thereafter that, the peaks shifted towards the higher frequency

side of the spectra on increasing the concentration of PEO₅ and PVDF. This spectra (Fig. 10) attribute to heterogenous segmental mobility due to PEO₅ and PVDF [57–59]. This heterogenous mobility is induced due to the high and low mobile components, different chain ends, and loop length of the polymers [58–60].

Conclusion

Novel blend solid polymer electrolyte (BSPE) systems were prepared by adding PEO₅ and PVDF into PEO₆ polymer matrix. The addition of PEO₅ and PVDF polymers enhanced the amorphous phase and structural dynamics of PEO₆ by creating extra free voids for lithium-ion mobility. The XRD and DSC results revealed that the presence of PEO₅ and PVDF polymers resulted in the reduction of crystalline nature of the samples at lower temperature (up to 303 K). FTIR data showed various changes in peak position, vibrational intensity, band width, and emergence and disappearance of peaks which confirmed the polymer-polymer and polymer-salt interactions. The ion transport numbers (> 0.9) indicate that the charge transport in these BSPE systems is mainly due to the movement of ions. The impedance data is analyzed using the equivalent electrical circuit which fits well with the experimental data. The optimal composition P3 (94 wt% PEO₆ + 3 wt% PEO₅ + 3 wt% PVDF with LiClO₄) exhibited lower crystallinity, melting temperature, and activation energy, with better hopping rate, ion concentration factor. These parameter lead to higher ionic conductivity value of $6.44 \times 10^{-4} \text{ Scm}^{-1}$ at 303 K which is one order higher than the similar systems reported elsewhere. The ionic conductivity studies on these BSPE systems obeyed the Arrhenius relationship and Jonscher's power law. Thus, the addition of PEO₅ and PVDF polymers to PEO₆ enhance the ionic conductivity of the BSPE systems, and such systems can be promising lithium conducting electrolytes for energy storage devices and other applications. However, there are several concerns and challenges related to BSPEs like, compatibility

and interfacial interaction between the polymers in the blend, achieving well controlled and uniform distribution of difference polymer components within the blend, coupled with, variation in molecular weight and chemical structure that can impact the overall stability and performance of the blend polymer electrolyte systems. Despite these critical opinions, studies have reported promising results which overcomes the limitations and harness the potential benefits of these complex BSPE systems.

Acknowledgements The author C. Revathy sincerely thanks PES University and Department of Science & Humanities (Physics) where the present research work was carried out.

Author contributions Conceptualization and methodology: Sunitha V R. Formal analysis and investigation: Sunitha V R, S. Radhakrishnan, and Rex Joseph. Material preparation and data collection: C Revathy. Data analysis: C Revathy, Sunitha V R, and Benson K Money. Original draft preparation: C Revathy. Review and editing: Sunitha V R, Benson K Money, and S. Radhakrishnan. Supervision: S. Radhakrishnan and Sunitha V R. All authors read and approved the final manuscript.

Data Availability Not applicable

Declarations

Ethical approval No experiments about human or animals were conducted.

Competing interests The authors declare no competing interests.

References

- Mallaiyah Y, Jeedi VR, Swarnalatha R et al (2021) Impact of polymer blending on ionic conduction mechanism and dielectric properties of sodium based PEO-PVdF solid polymer electrolyte systems. *J Phys Chem Solids* 155:110096. <https://doi.org/10.1016/j.jpms.2021.110096>
- Sundar M, Selladurai S (2006) Effect of fillers on magnesium-poly(ethylene oxide) solid polymer electrolyte. *Ionics (Kiel)* 12:281–286. <https://doi.org/10.1007/s11581-006-0048-9>
- Wang J, Fan L, Du Q, Jiao K (2022) Lithium ion transport in solid polymer electrolyte filled with alumina nanoparticles. *Energy Adv* 1:269–276. <https://doi.org/10.1039/d2ya00025c>
- Basappa M, Ganesha H, Veeresh S et al (2022) Preparation, characterization, and electrochemical properties of PEO/PVDF blend films. *Chem Phys Lett* 799:139609. <https://doi.org/10.1016/j.cplett.2022.139609>
- Li J, Zhu K, Yao Z et al (2020) A promising composite solid electrolyte incorporating LLZO into PEO/PVDF matrix for all-solid-state lithium-ion batteries. *Ionics (Kiel)* 26:1101–1108. <https://doi.org/10.1007/s11581-019-03320-x>
- Sundaramahalingam K, Muthuvinayagam M, Nallamuthu N (2019) AC impedance analysis of lithium ion based PEO:PVP solid polymer blend electrolytes. *Polym Sci - Ser A* 61:565–576. <https://doi.org/10.1134/S0965545X19050171>
- Baskaran R, Selvasekarapandian S, Kuwata N et al (2006) ac impedance, DSC and FT-IR investigations on (x)PVAc-(1-x) PVdF blends with LiClO₄. *Mater Chem Phys* 98:55–61. <https://doi.org/10.1016/j.matchemphys.2005.08.063>
- Natarajan R, Subramanian S, Moni P, Karthikeyan Shunmugavel S (2013) Lithium ion conducting solid polymer blend electrolyte based on bio-degradable polymers. *Bull Mater Sci* 36:333–339. <https://doi.org/10.1007/s12034-013-0463-2>
- Sengwa RJ, Choudhary S, Dhatarwal P (2019) Investigation of alumina nanofiller impact on the structural and dielectric properties of PEO/PMMA blend matrix-based polymer nanocomposites. *Adv Compos Hybrid Mater* 2:162–175. <https://doi.org/10.1007/s42114-019-00078-8>
- Yu X, Manthiram A (2020) A long cycle life, all-solid-state lithium battery with a ceramic-polymer composite electrolyte. *ACS Appl Mater Interfaces*. <https://doi.org/10.1021/acsami.9b02547>
- Caradant L, Lepage D, Nicolle P et al (2020) Blend of polymers as new solid electrolytes for lithium-ion batteries. *ECS Meet Abstr MA2020-02:896–896*. <https://doi.org/10.1149/ma2020-025896mtgabs>
- Otsugu S, Kimura Y, Nakajima H, Loos K (2020) Enhancement of T_g of poly(l-lactide) by incorporation of biobased mandelic-acid-derived phenyl groups by polymerization and polymer blending. *Macromol Chem Phys* 221:1900392. <https://doi.org/https://doi.org/10.1002/macp.201900392>
- Dhatarwal P, Sengwa RJ (2019) Polymer compositional ratio-dependent morphology, crystallinity, dielectric dispersion, structural dynamics, and electrical conductivity of PVDF/PEO blend films. *Macromol Res* 27:1009–1023. <https://doi.org/10.1007/s13233-019-7142-0>
- Dhatarwal P, Sengwa RJ (2019) Impact of PVDF/PEO blend composition on the β-phase crystallization and dielectric properties of silica nanoparticles incorporated polymer nanocomposites. *J Polym Res* 26. <https://doi.org/10.1007/s10965-019-1859-5>
- Mahendran O, Chen SY, Chen-Yang YW et al (2005) Investigations on PMMA-PVdF polymer blend electrolyte with esters of dibenzoic acids as plasticizers. *Ionics (Kiel)* 11:251–258. <https://doi.org/10.1007/BF02430385>
- Ngai KS, Ramesh S, Ramesh K, Juan JC (2016) A review of polymer electrolytes: fundamental, approaches and applications. *Ionics (Kiel)* 22:1259–1279. <https://doi.org/10.1007/s11581-016-1756-4>
- Rajendran S, Sivakumar P (2008) An investigation of PVdF/PVC-based blend electrolytes with EC/PC as plasticizers in lithium battery applications. *Phys B Condens Matter* 403:509–516. <https://doi.org/10.1016/j.physb.2007.06.012>
- Ndruru STCL, Wahyuningrum D, Bundjali B, Arcana IM (2020) Preparation and characterization of biopolymer electrolyte membranes based on liclo4-complexed methyl cellulose as lithium-ion battery separator. *J Eng Technol Sci* 52:28–50. <https://doi.org/https://doi.org/10.5614/j.eng.technol.sci.2020.52.1.3>
- Hirankumar G, Mehta N (2018) Effect of incorporation of different plasticizers on structural and ion transport properties of PVA-LiClO₄ based electrolytes. *Heliyon* 4. <https://doi.org/10.1016/j.heliyon.2018.e00992>
- Stephan AM (2006) Review on gel polymer electrolytes for lithium batteries. *Eur Polym J* 42:21–42. <https://doi.org/10.1016/j.eurpolymj.2005.09.017>
- Xu J, Liu Y, Cao Q et al (2019) A high-performance gel polymer electrolyte based on poly(vinylidene fluoride)/thermoplastic polyurethane/poly(propylene carbonate) for lithium-ion batteries. *J Chem Sci* 131:49. <https://doi.org/10.1007/s12039-019-1627-4>
- Ueno M, Imanishi N, Hirano A et al (2009) Effect of molecular weight in composite polymer electrolyte for all solid lithium polymer battery. *ECS Meet Abstr MA2009-02:574–574*. <https://doi.org/10.1149/MA2009-02/8/574>
- Abutalib MM, Rajeh A (2020) Influence of Fe₃O₄ nanoparticles on the optical, magnetic and electrical properties of PMMA/PEO composites: Combined FT-IR/DFT for electrochemical applications. *J Organomet Chem* 920:3–10. <https://doi.org/10.1016/j.jorganchem.2020.121348>

24. Prasanth R, Shubha N, Hng HH, Srinivasan M (2013) Effect of nano-clay on ionic conductivity and electrochemical properties of poly(vinylidene fluoride) based nanocomposite porous polymer membranes and their application as polymer electrolyte in lithium ion batteries. *Eur Polym J* 307–318. <https://doi.org/10.1016/j.eurpolymj.2012.10.033>
25. Sunitha VR, Radhakrishnan S (2016) Impedance and dielectric studies of nanocomposite polymer electrolyte systems using MMT and ferroelectric fillers. *Ionics (Kiel)* 22:2437–2446. <https://doi.org/10.1007/s11581-016-1784-0>
26. Zhao J, Wang L, He X et al (2008) Determination of lithium-ion transference numbers in LiPF₆[sub 6]–PC solutions based on electrochemical polarization and NMR measurements. *J Electrochem Soc* 155:A292. <https://doi.org/10.1149/1.2837832>
27. Zugmann S, Fleischmann M, Amereller M et al (2011) Measurement of transference numbers for lithium ion electrolytes via four different methods, a comparative study. *Electrochim Acta* 56:3926–3933. <https://doi.org/10.1016/j.electacta.2011.02.025>
28. Son CY, Wang Z-GG (2020) Ion transport in small-molecule and polymer electrolytes. *J Chem Phys* 153:100903. <https://doi.org/10.1063/5.0016163>
29. Chen P, Liang X, Wang J et al (2017) PEO/PVDF-based gel polymer electrolyte by incorporating nano-TiO₂ for electrochromic glass. *J Sol-Gel Sci Technol* 81:850–858. <https://doi.org/10.1007/s10971-016-4235-5>
30. Maheshwaran C, Mishra K, Kanchan DK, Kumar D (2020) Mg²⁺ conducting polymer gel electrolytes: physical and electrochemical investigations. *Ionics (Kiel)* 26:2969–2980. <https://doi.org/10.1007/s11581-020-03459-y>
31. Elashmawi IS, Ismail AM (2022) Study of the spectroscopic, magnetic, and electrical behavior of PVDF/PEO blend incorporated with nickel ferrite (NiFe₂O₄) nanoparticles. *Polym Bull.* <https://doi.org/10.1007/s00289-022-04139-9>
32. Choudhary S, Sengwa RJ (2017) Effects of different inorganic nanoparticles on the structural, dielectric and ion transportation properties of polymers blend based nanocomposite solid polymer electrolytes. *Electrochim Acta* 247:924–941. <https://doi.org/10.1016/j.electacta.2017.07.051>
33. Kuila T, Acharya H, Srivastava SK et al (2007) Enhancing the ionic conductivity of PEO based plasticized composite polymer electrolyte by LaMnO₃ nanofiller. *Mater Sci Eng B Solid-State Mater Adv Technol* 137:217–224. <https://doi.org/10.1016/j.mseb.2006.11.023>
34. Sunitha VR, Radhakrishnan S (2015) Field enhanced Li ion conduction in nanoferroelectric modified polymer electrolyte systems. *Ionics (Kiel)* 21:949–954. <https://doi.org/10.1007/s11581-014-1252-7>
35. Ranjana PAB, Sundaresan B (2020) A study on the complex formation of poly(methyl methacrylate), poly(vinyl chloride) and their blend with lithium perchlorate using FTIR spectroscopy. *Macromol Symp* 392:3–6. <https://doi.org/10.1002/masy.202000172>
36. Kumar D, Hashmi SA (2010) Ion transport and ion-filler-polymer interaction in poly(methyl methacrylate)-based, sodium ion conducting, gel polymer electrolytes dispersed with silica nanoparticles. *J Power Sources* 195:5101–5108. <https://doi.org/10.1016/j.jpowsour.2010.02.026>
37. Kumar KK, Ravi M, Pavani Y et al (2012) Electrical conduction mechanism in NaCl complexed PEO/PVP polymer blend electrolytes. *J Non Cryst Solids* 358:3205–3211. <https://doi.org/10.1016/j.jnoncrysol.2012.08.022>
38. Aziz SB, Abidin ZHZ (2013) Electrical conduction mechanism in solid polymer electrolytes: new concepts to Arrhenius equation. *J Soft Matter* 2013:1–8. <https://doi.org/10.1155/2013/323868>
39. Sengwa RJ, Sankhla S, Choudhary S (2010) Effect of melt compounding temperature on dielectric relaxation and ionic conduction in PEO–NaClO₄–MMT nanocomposite electrolytes. *Ionics (Kiel)* 16:697–707. <https://doi.org/10.1007/s11581-010-0453-y>
40. Shanmukaraj D, Wang GX, Murugan R, Liu HK (2008) Ionic conductivity and electrochemical stability of poly(methylmethacrylate)-poly(ethylene oxide) blend-ceramic fillers composites. *J Phys Chem Solids* 69:243–248. <https://doi.org/10.1016/j.jpcs.2007.08.072>
41. Dannoun EMA, Aziz SB, Brza MA et al (2022) Electrochemical and Ion transport studies of Li⁺ ion-conducting MC-based biopolymer blend electrolytes. *Int J Mol Sci* 23:1–16. <https://doi.org/10.3390/ijms23169152>
42. Sunitha VR, Radhakrishnan S (2020) Gamma irradiation effects on conductivity and dielectric behaviour of PEO-based nano-composite polymer electrolyte systems. *Polym Bull* 77:655–670. <https://doi.org/10.1007/s00289-019-02770-7>
43. Wang W, Alexandridis P (2016) Composite polymer electrolytes: nanoparticles affect structure and properties. *Polymers (Basel)* 8. <https://doi.org/10.3390/polym8110387>
44. Money BK, Hariharan K (2010) Phase dependent heterogeneous dynamics of Li⁺ Ion in LiPO₃ based systems. *Integr Ferroelectr* 120:75–89. <https://doi.org/10.1080/10584587.2010.491729>
45. Ahmad MM, Al-Jaafari A (2015) Concentration and mobility of mobile Li⁺ ions in Li₆BaLa₂Ta₂O₁₂ and Li₅La₃Ta₂O₁₂ garnet lithium ion conductors. *J Mater Sci Mater Electron* 26:8136–8142. <https://doi.org/10.1007/s10854-015-3473-6>
46. Money BK, Hariharan K, Swenson J (2012) Glass transition and relaxation processes of nanocomposite polymer electrolytes. *J Phys Chem B* 116:7762–7770. <https://doi.org/10.1021/jp3036499>
47. Sindhu KP, Abdul Majeed SSM, Shahitha Parveen J (2021) PEO/PMMA solid nanocomposite polyelectrolyte with enhanced ionic conductivity and promising dielectric properties. *J Electron Mater* 50:6654–6666. <https://doi.org/10.1007/s11664-021-09205-y>
48. Liang B, Tang S, Jiang Q et al (2015) Preparation and characterization of PEO-PMMA polymer composite electrolytes doped with nano-Al₂O₃. *Electrochim Acta* 169:334–341. <https://doi.org/10.1016/j.electacta.2015.04.039>
49. Yap YL, You AH, Teo LL (2019) Preparation and characterization studies of PMMA–PEO-blend solid polymer electrolytes with SiO₂ filler and plasticizer for lithium ion battery. *Ionics (Kiel)* 25:3087–3098. <https://doi.org/10.1007/s11581-019-02842-8>
50. Teran AA, Tang MH, Mullin SA, Balsara NP (2011) Effect of molecular weight on conductivity of polymer electrolytes. *Solid State Ionics* 203:18–21. <https://doi.org/10.1016/j.ssi.2011.09.021>
51. Knoglinger H, Schausberger A, Janeschitz-Kriegl H (1987) The role of short chain molecules for the rheology of polystyrene melts. - I. Molar mass dependent shift factors. *Rheol Acta* 26:460–467. <https://doi.org/10.1007/BF01333847>
52. Singh KP, Gupta PN (1998) Study of dielectric relaxation in polymer electrolytes. *Eur Polym J* 34:1023–1029. [https://doi.org/10.1016/S0014-3057\(97\)00207-3](https://doi.org/10.1016/S0014-3057(97)00207-3)
53. Choudhary S (2017) Structural and dielectric properties of (PEO–PMMA)–SnO₂ nanocomposites. *Compos Commun* 5:54–63. <https://doi.org/10.1016/j.coco.2017.07.004>
54. Perera K, Vidanapathirana K (2017) Impedance spectroscopy, DC polarization, XRD and SEM studies on an ionic liquid based gel polymer electrolyte to be used for dye sensitized solar cells. *Mater Discov* 7:30–33. <https://doi.org/10.1016/j.md.2017.07.002>
55. Dutta P, Biswas S, De Kumar S (2002) Dielectric relaxation in polyaniline-polyvinyl alcohol composites. *Mater Res Bull* 37:193–200. [https://doi.org/10.1016/S0025-5408\(01\)00813-3](https://doi.org/10.1016/S0025-5408(01)00813-3)
56. Aziz BM, Brza et al (2019) Employing of Trukhan model to estimate ion transport parameters in PVA based solid polymer electrolyte. *Polymers (Basel)* 11:1694. <https://doi.org/10.3390/polym11101694>
57. Jayathilaka PARD, Dissanayake MAKL, Albinsson I, Mellander BE (2003) Dielectric relaxation, ionic conductivity and thermal studies of the gel polymer electrolyte system PAN/EC/PC/LiTFSI. *Solid State Ionics* 156:179–195. [https://doi.org/10.1016/S0167-2738\(02\)00616-1](https://doi.org/10.1016/S0167-2738(02)00616-1)

58. Alegria A, Colmenero J (2016) Dielectric relaxation of polymers: segmental dynamics under structural constraints. *Soft Matter* 12:7709–7725. <https://doi.org/10.1039/c6sm01298a>
59. Chu L, Xu K, Graf R et al (2021) Dynamic heterogeneity in homogeneous polymer melts. *Soft Matter* 17:6081–6087. <https://doi.org/10.1039/d1sm00017a>
60. Metin B, Blum FD (2006) Segmental dynamics in poly(methyl acrylate) on silica: molecular-mass effects. *J Chem Phys* 125. <https://doi.org/10.1063/1.2219739>

Publisher's note Springer Nature remains neutral with regard to jurisdictional claims in published maps and institutional affiliations.

Springer Nature or its licensor (e.g. a society or other partner) holds exclusive rights to this article under a publishing agreement with the author(s) or other rightsholder(s); author self-archiving of the accepted manuscript version of this article is solely governed by the terms of such publishing agreement and applicable law.